Two views of the Martian North Polar Layered Deposits: Toward a correlation of radar and visible stratigraphic records

P. Becerra[1], D. Nunes[2], I.B. Smith[3,4], M.M. Sori[5], N. Thomas[1]; [1]Physikalisches Institut, Universität Bern, Switzerland, [2]Jet Propulsion Laboratory, Pasadena, USA. [3]Planetary Science Institute, Colorado, USA, [4]York University, Toronto, Ontario, Canada. [5]University of Arizona, Tucson, USA.

Introduction: A long-standing problem in Mars Polar Science is the interpretation of the stratigraphic record preserved in Mars' icy North Polar Layered Deposits (NPLD) [1] (Fig. 1a), whose accumulation patterns of ice and dust are associated with recent climate change forced by variations in the planet's astronomical parameters [2]. The internal bedding is visible from orbit in exposures within spiraling troughs that dissect the NPLD dome (Fig. 1a,b). Studies have used images of these troughs to map the stratigraphy [3-6] and describe links between NPLD accumulation and astronomical forcing [7-10]. Sub-surface radar sounding also observes this internal structure. The Shallow Radar (SHARAD) [11] detects changes in dielectric properties with depth. As these vary for layers with different amounts of dust, layering is observed as "reflector" surfaces [12].

The optical and radar-based stratigraphies have predominantly been studied in isolation. In terrestrial climate science [13], orbital climate forcing was confirmed by correlation of sedimentary, geochemical and paleo-magnetic records, suggesting that integration of datasets is key to understanding the record in the NPLD. In general, both radar and optical layers are assumed to result from varying amounts of dust in the ice [14,15], but differences in vertical resolution have prevented 1-to-1 correlation.

Here, we test the hypothesis that highly protruding 'Marker Beds (MBs)' have sufficient dielectric contrast with neighboring beds to create radar reflections. If true, this would associate individual reflectors to exposed beds, allowing for dust/ice columns based on the combined data, which could constrain orbitally-forced accumulation models [16,17] to decipher the climate record of the NPLD.

Methods: Becerra et al. [8] mapped the stratigraphy of the NPLD by identifying sequences of MBs in "protrusion profiles" of bed exposures in troughs made from HiRISE [18] Digital Terrain Models (DTMs; [19]), and correlating these from different locations (Fig. 1; [8]). Protrusion is a proxy for resistance to erosion and is calculated by measuring the difference between the topography of a trough wall, and a linear fit to the wall within a certain window (Fig. 1a). A protrusion profile for site N0 is shown in Fig. 2b. With these data, our approach to correlation is a 4-step process:

(1) Average SHARAD data near the exposures to obtain representative radargrams. The variability of the SHARAD response within small regions of interest (ROIs) next to exposure sites is not negligible. To assess this, we selected segments of three SHARAD radar tracks that fall within a 3 km ROI near a study site, and averaged all soundings in each segment (Fig. 2a,c). This is representative of the variations in radar response within the ROI.

(2) Compare average radargrams directly to the protrusion profiles of [8] to search for an MB-reflector correlation. For this, we subtract the linear attenuation in the data and normalize all quantities to mean = 0 and variance = 1. We then search for the maximum cross-correlation between protrusion profiles and average radargrams. This is shown in Fig 2d.

(3) Model the radar wave propagation [14] through synthetic permittivity (ε') profiles, which are constrained by the best-fit correlations from step 2. MBs translate into layers of varying ε depending on their initial correlation with the radargram. We can then compare the model radargrams to the real ones at each location. We tested a preliminary model, selecting the MBs from the N0 profile that appeared to fit the radar peaks and assigning them $\varepsilon' = 4$ over a water ice background with $\varepsilon' = 3.12$. Fig. 2e shows the dielectric profile modeled after the protrusion profile of site N0, and Fig. 2f shows the resulting simulated radargram.

(4) Correlate the simulated radargrams to real SHARAD data using spectral analysis and pattern-matching algorithms. This correlation will result in representative HiRISE/SHARAD-based stratigraphic columns of ε', which can be transformed to fractional dust-content [20,21] that can serve as virtual ice cores and be used to constrain accumulation models.

Preliminary Results: Results of the cross-correlation of SHARAD with the protrusion profiles for sites N0, N2, and N11 are shown in Fig 3. For the direct cross-correlation with protrusion we select only the sections of the radargrams that correspond to the estimated relevant depth range [~2–8 μs]. For N0, we also ran a comparison with the preliminary model results. All three sites show a relatively good correlation between peaks in each data profile, but some peaks in the radargram match troughs in protrusion instead. However, radar reflections represent interfaces between materials of different ε', so it is not implausible that a transition to a low-dust, less-protruding layer would also produce a relatively strong reflection. Although the direct protrusion-radar comparison at N0 shows promising results, the model radargram-to-real-radargram comparison at this same site appears to have lost the correlation. More work is

needed in the model radargrams to be able to produce representative multi-data columns.

Conclusions and Future Work: Beds of high protrusion appear to match radar reflectors at three sites. An attempted correlation at site N6 failed at the first stage however, and the model at N0 does not show the expected correlation with the real radargram. We must study all geometrically favourable locations and test for statistical significance at each one. In addition, we will use the correlations with protrusion to inform the model and then use Dynamic Time Warping [7,22] to tune the model and find the best-fit dielectric profile at each site. The final step of the work will be to transform these profiles into dust/ice ratio columns [20,21] for use as input on accumulation models [17]. Naturally, a higher spatial-resolution radar in orbit around Mars would greatly improve the chances of subsurface-surface integration. Such an instrument is being proposed as a NASA Discovery mission [23], and this work can help predict the results that would be returned.
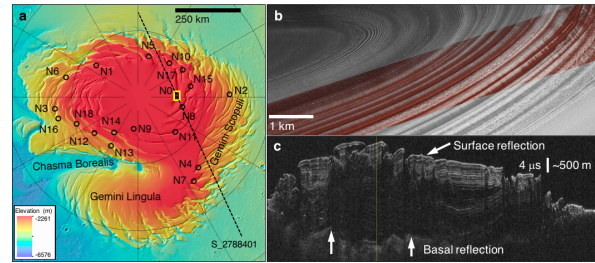

Figure 1. (a) Topographic map of the NPLD. Circles = locations of sites with HiRISE DTMs. Line = ground track of SHARAD radargram in (c). **(b)** HiRISE image of exposed layers in the N0 trough from (a). **(c)** SHARAD radargram 2788401. Yellow line marks the approximate location of N0.
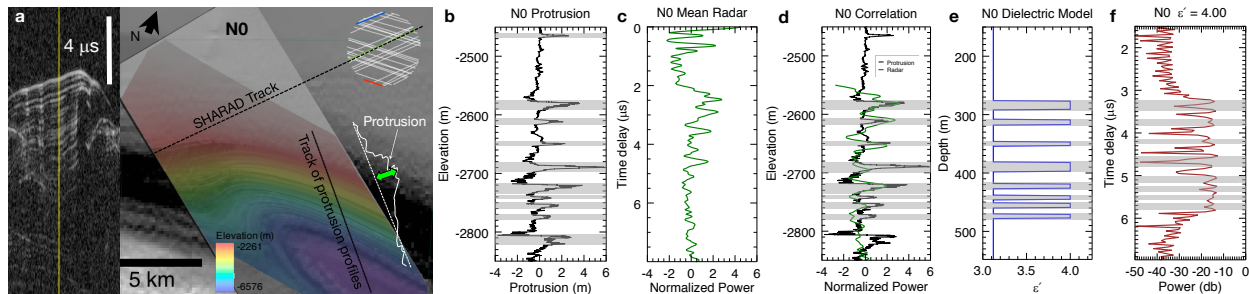

Figure 2. Preliminary radar-protrusion correlation. **(a)** SHARAD radargram (left) and HiRISE DTM (right) of site N0 from Fig.1a. Yellow line on the radargram indicates approximate location of the circular ROI on the top right, which shows the tracks of all soundings that were averaged to produce the mean radar profile. **(b)** Protrusion profile. Protruding beds are shaded in grey. The green arrow in the diagram in (a) explains the calculation of protrusion schematically. **(c)** Mean radar profile. **(d)** Cross-correlation of protrusion to radar profiles. Here, grey shading indicates protruding beds matched to radar reflectors. **(e)** Synthetic dielectric column assuming matched beds are dust-rich (ε' = 4). **(f)** Simulated radar profile generated by propagating a radar pulse through the column in (e).
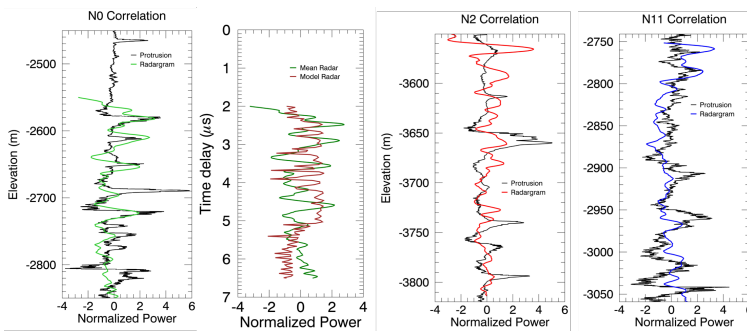

Figure 3. From left to right: Direct cross-correlation of mean N0 radargram with protrusion, cross-correlation between N0 model and mean radargram, cross-correlation of mean N2 radargram with protrusion, and the same for N11

References
[1] Smith, et al. Icarus (2017) [2] Cutts, et al. Science (1976) [3] Fishbaugh et al. (2006) [4] Fishbaugh et al. GRL (2010) [5] Limaye et al. JGR (2012) [6] Becerra et al. JGR (2016) [7] Laskar et al. Nature (2002) [8] Milkovich and Head, JGR (2005) [9] Perron and Huybers, Geology (2009) [10] Becerra et al. GRL (2017) [11] Seu et al. JGR (2007) [12] Putzig et al. Icarus (2009) [13] Imbrie, Icarus (1982) [14] Nunes & Phillips, JGR (2006) [15] Christian, et al. Icarus (2013) [16] Levrard et al. JGR (2007) [17] Hvidberg et al. Icarus (2012) [18] McEwen et al. JGR (2007) [19] Kirk et al. JGR (2008) [20] Stillman, et al. J.Phys.Chem. (2010) [21] Brouet et al. Icarus (2018) [22] Sori et al. Icarus (2014). [23] Byrne et al. this conference.